AAS 11-267

PARAMETER VARIATION IN NEAR-EARTH OBJECT DISRUPTION SIMULATIONS USING GPU ACCELERATION

Brian D. Kaplinger* and Bong Wie†

This paper focuses on the problem of disrupting a Near-Earth Object (NEO) on terminal approach with the Earth, investigating the effects of changing explosive power and timing the fragmentation to coincide with orbital dispersion properties. Simulation and analysis of previous results have shown that fragmenting and dispersing a hazardous NEO could lower the total mass impacting the Earth for some orbits. The problem is simulated numerically using the computational capabilities of a Graphics Processing Unit (GPU) to accelerate calculations and enable variation of several mission and orbital parameters. Model upgrades and higher resolution simulation capabilities are demonstrated for an Apophis-like orbit. Unique benefits and limitations to the GPU architecture are discussed, and preliminary results equivalent to months of serial computation are presented.

INTRODUCTION

This section describes the motivation behind the Near-Earth Object (NEO) disruption problem, and the desire to accelerate present simulation models using Graphics Processing Units (GPUs). It also presents the concerns (both technical and political) levied against the use of nuclear explosions to demonstrate the capabilities necessary to disrupt (i.e. fragment and disperse) an NEO.

Asteroid Deflection

With thousands of known NEOs crossing the orbit of Earth, and over 1100 of these considered potentially hazardous at this time [1], there has been significant scientific interest in developing the capability to deflect an NEO from an impacting trajectory. Conventional wisdom, and a substantial amount of planetary defense literature, has held that the best way to accomplish this goal is to slowly push the NEO onto another trajectory, or to use an impulsive force (nuclear standoff explosion or kinetic impactor) at least a decade in advance of impact [2, 3]. Two main motives drive research into high-energy, last minute options for asteroid deflection: a) Many bodies on impacting trajectories may not be detected early enough to spend decades deflecting their orbits, and b) The expense and risk of an interplanetary mission to deflect an NEO will require that an object be demonstrated to pose a substantial and imminent threat before action is taken.

While the “late notice” motive is becoming less relevant as more NEOs are catalogued, there are still small bodies that are detected within weeks of closest approach [4], and it would be hard to prove that no more such bodies exist. The “late decision” motive is a political and fiscal reality that planetary defense researchers will have to consider. Even if a viable method of deflection is demonstrated and awaits deployment, a potential target must be shown to impact the Earth considering all relevant uncertainties. As the long-term ephemerides of a small body in the solar system contain many uncertainties that could account for several Earth radii of displacement [5, 6], we expect that a decision to deflect an NEO will come within the last few orbits before impact (possibly after a close approach with the Earth alters the body trajectory).

*Graduate Assistant, Asteroid Deflection Research Center, Iowa State University, 2271 Howe Hall, Room 2355, Ames, IA, 50011-2271, bdkaplin@iastate.edu.
†Vance Coffman Endowed Chair Professor, Asteroid Deflection Research Center, Iowa State University, 2271 Howe Hall, Room 2355, Ames, IA, 50011-2271, bongwie@iastate.edu.

The asteroid 99942 Apophis is one such example. Initially given a much higher probability of impact on April 13, 2036, the current estimated probability of impact is 1 out of 250,000 after many additional observations. There is still much uncertainty of what will happen after Apophis passes within 36,000 km of the Earth on April 13, 2029 [7]. If a body like Apophis was forced into a resonant orbit after a close approach with the Earth and was confirmed to be on an impacting trajectory, we would only have a short window in which to act (7 years in the Apophis scenario). This has been shown to be problematic for mission design, with reasonable launch windows only giving a few weeks of time for a deflection to take place [8].

Past research has shown that the use of a kinetic impactor or nuclear explosive device will possibly exceed the gravitational binding energy of many NEOs during a deflection attempt [9]. Additionally, it has been shown that fragmenting an Apophis-like body on an impacting trajectory can reduce the amount of impacting mass remaining on impacting trajectories to 1% in as little as 15 days [6,10], a scenario in which some amount of impacting mass is inevitable. Modeling of atmospheric reentry for a fragmented body has suggested that lowering the individual masses results in substantial reduction of ground impacts, with many fragments burning up or being partially ablated by the atmosphere [6]. Therefore, it is desired that any viable last-minute option lower the impacting mass below this threshold, allowing the atmosphere to have an increased effect. For this reason, we investigate the timing of NEO fragmentation and the scaling of initial explosive energy to model NEO disruption and determine a desired course of action in a "late notice" or "late decision" scenario.

GPU Computing

As the Central Processing Unit (CPU) of the modern personal computers and workstations evolved, there was a substantial problem overcoming thermal issues that accompanied additional computing power. One solution to these thermal issues was to design multi-core CPUs capable of handling several computing threads in parallel [11]. Additionally, as graphics for games and commercial applications grew more demanding, a separate Graphics Processing Unit (GPU) was implemented to allow the screen rendering to be performed by an alternate processing chip. In most graphic applications, either pixels or sections of the display can be calculated separately from each other. Due to this fact, the GPU evolved into a many-core parallel structure, trading core clock speed for number of parallel computing threads. At the time of writing, retail GPU chips are available with up to 512 cores and over 1 trillion floating point operations per second (FLOPs) of theoretical computing power [11, 12]. For comparison, a standard workstation processor averages 10-20 GFLOPs. Due to this leap in technology, the GPU has been considered by many the ideal commercially-available massively parallel architecture.

Early simulations and computing programs written for execution on the GPU were done using graphics processing languages. These approaches cleverly harnessed the computing power available by casting a problem as one involving textures and pixels. DirectCompute, OpenGL, and other languages were very powerful methods for moving computation from the CPU to the GPU, freeing resources and allowing problems to scale more easily [13]. However, for general scientific computing this method had a steep learning curve. In 2006, NVIDIA launched the Compute Unified Device Architecture (CUDA), which allowed compilation of GPU executables to be created through extensions to the C language. This approach is highly portable, and an example of the versatility of general scientific computing on the GPU [12]. The CUDA C approach will be the method discussed in this paper.

PROBLEM FORMULATION

This section describes the underlying problem being solved. A model of the fragmentation due to the subsurface detonation of an explosive is briefly outlined. We present previous results describing the behavior of this model to scaling of explosive energy and timing along the orbit. The general formulation of the orbit propagation model used is discussed, followed by the model used for atmospheric reentry.

Subsurface Explosion Model

The hypothetical deflection mission target presented in this paper is an NEO with a total mass of 2.058E10 kg and a diameter of 270 meters, as shown in Figure 1. A full description of the construction of this Apophis-like model can be found in [14]. A nuclear explosion equivalent to 300 kT was simulated in a cylindrical region below the surface of the body, creating a shock that propagates through the body resulting in fragmentation and dispersal. The core region was modeled with a linear strength model and a yield strength of 14.6 MPa. The mass-averaged speed of the fragments after 6 seconds was near 50 m/s with peak near 30 m/s, as shown in Figure 2. Figure 2 also shows the axisymmetric distribution of body fragments after the completion of the subsurface explosion simulation.

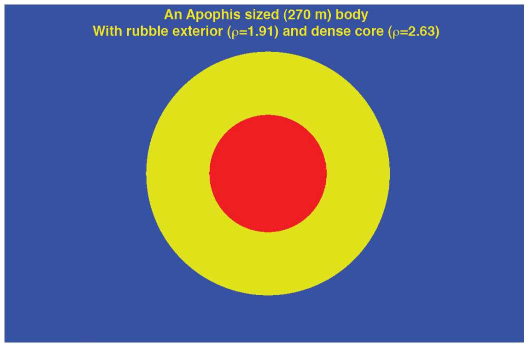
An Apophis sized (270 m) body
With rubble exterior (ρ=1.91) and dense core (ρ=2.63)

Figure 1. Structural Model of an Apophis-sized (270 m) Body [10].

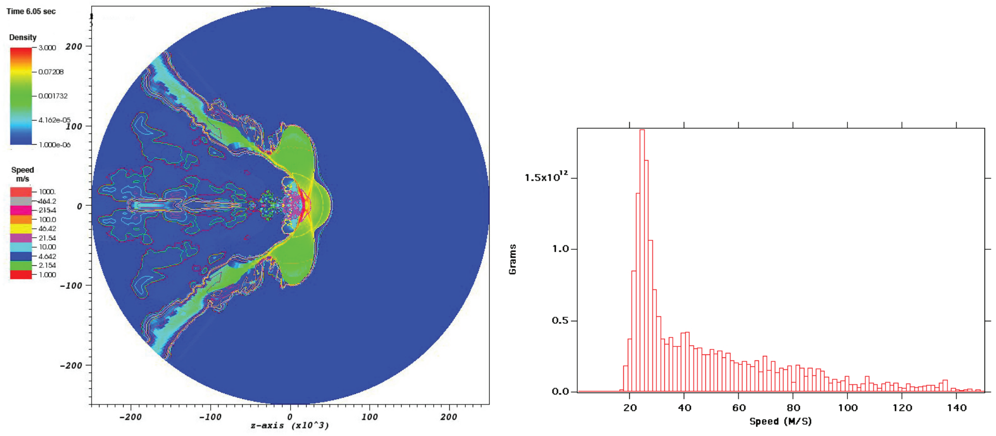

Figure 2. Distribution of Fragments and Velocities for 300 kT Subsurface Explosion [10].

A three-dimensional fragment distribution was constructed by Dr. David Dearborn at Lawrence Livermore National Laboratory from the hydrodynamics model by rotating the state variables about the axis of symmetry, resulting in particle state values for a reasonable NEO fragmentation. To track the dispersion of these fragments along the orbital trajectory before impact, the relative position axes were aligned such that the highest momentum projectiles coincided with the desired deflection direction at the time of the explosion. A velocity scaling parameter allows the testing of distributions with fragment velocities different than the predicted 50 m/s maximum velocity from the explosion simulation.

Previous Scaling and Timing Results

Previous model results [6] focused on individually varying parameters of the simulation to gauge their representative importance. It was found that orientation of the explosion direction was extremely important to overall mission effectiveness. Dispersion along the orbital track, while a common method proposed for long term deflection, results in 26.1% of the initial mass on impacting trajectories after 15 days. Dispersion along the radial direction (outwards from the Sun) was found to be near-optimal for an Apophis-like orbit, with only 0.6% of the initial NEO mass remaining to impact the Earth. A comparison of close approach histograms for these two cases is shown in Figure 3.

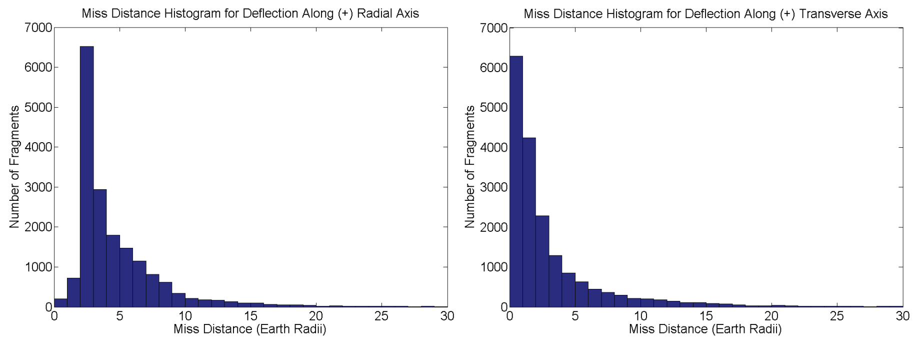

Figure 3. Miss Distance Histograms After 15 Day Orbital Dispersion [6].

Basic reentry modeling of the falling fragments reduced both these estimates by around 80%, assuming that all bodies were made of the denser core material. However, it was suggested that distance between atmospheric reentry events, both in distance and time, is desirable to minimize shared bow shocks during reentry. Therefore, we conclude that a well dispersed pattern of reentry events is desirable. Figure 4 shows one such example of a desired pattern, with fragments entering the atmosphere over the course of 5 hours in widely spaced locations.

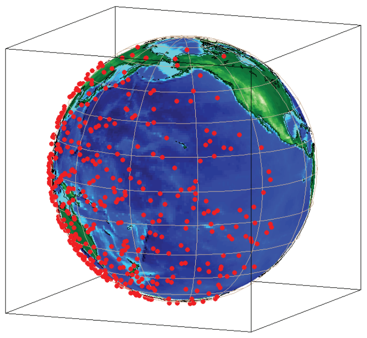

Figure 4. Impact Locations on a Fixed Earth after Radial Deflection [6].

Two distinct parameters were investigated in previous results and the present paper. The first parameter is a scaling of the initial velocity of the fragmented system corresponding to varying the explosive energy used. The second parameter is shifting the timing of the dispersion to a specific point before impact. The nominal case discussed above uses initial kinetic energy corresponding to a 300 kT explosion and begins 15 days prior to the predicted impact. Reference [6] shows that in the case of a transverse (perpendicular to radial in the flight direction) deflection, increased dispersion time can be substantially more effective in reducing impacting mass than increased explosive energy. The first scaled almost linearly up to 25 days of lead time, while the latter scaled as exponential decay with additional energy. This result can be seen in Figure 5.

Since both parameters can have a substantial effect, and mission design is not limited to a few test cases, effective mission profiles can take advantage of known coupling between these two effects. Changing the

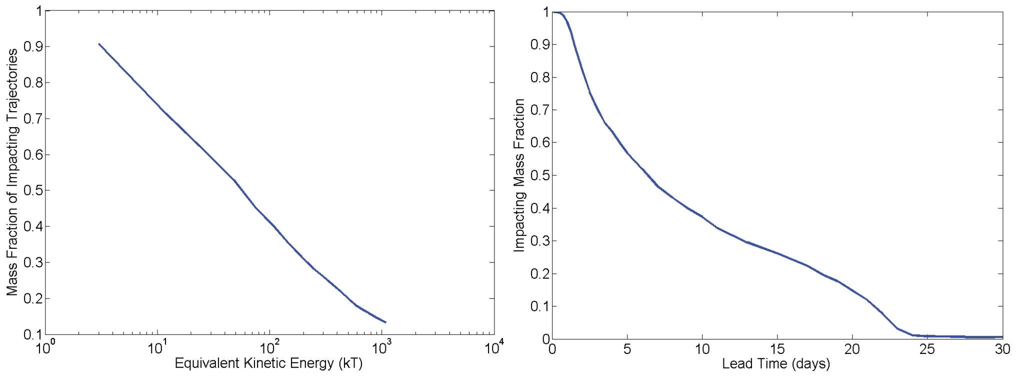

Figure 5. Impacting Mass Fractions from Initial Velocity Scaling and Timing Variation for Transverse Deflection.

timing directly feeds back to mission feasibility and scheduling, affecting the needed fuel and path for the intercepting spacecraft. Changing the explosive payload results in a spacecraft mass change, which can alter the end cost of the mission. Additionally, the feasibility of using conventional explosives (very low yield) for a proof-of-concept mission is of great interest. Provided the lower yield is able to sufficiently fragment the body, we desire a timing tradeoff that allows observation of mission success in a reasonably short period of time (2-3 months). After this time, perturbations to the orbit could substantially change the dispersion pattern from that initiated by the explosion. This coupling effect of timing and scaling is the primary motivation of the present work.

Orbit Propagation Model

In order to have a nominal impacting trajectory that is independent of platform and integration scheme, the present model computes the orbital parameters at the start of the simulation. These parameters are functions of the lead time before impact and are based on an estimated post-2029 orbit of the asteroid Apophis, assuming passage through a resonant keyhole orbit. Since the orbit is calculated at run time using the adaptive method described in [6,10], it also allows for changes to the orbital perturbations used in the model without sacrificing precision. The orbit used for a 15 day lead time impact is shown in Table 1.

Table 1. Orbital Parameters for 15 Day Impact Trajectory

Orbital Parameter	Value
Semimajor Axis	1.1082428 AU
Eccentricity	0.189928428
Inclination	2.18995362 deg
Longitude of Right Ascension	203.18642266 deg
Argument of Perihelion	69.929774 deg
Initial Mean Anomaly	296.74684241 deg
Epoch	64781 MJD
Miss Distance on Target Date	4.738466849E-011 Earth Radii

As described in [6], the present model computes the change of each fragment relative to the mean motion around the sun. Therefore, the nonlinear relative equations of motion are integrated to update the state of each fragment compared to a rotating coordinate system in orbit around the Sun (shown in Figure 6). Including the gravitational perturbations of the major planets, minor planets, and Earth's moon, the equations of motion are:

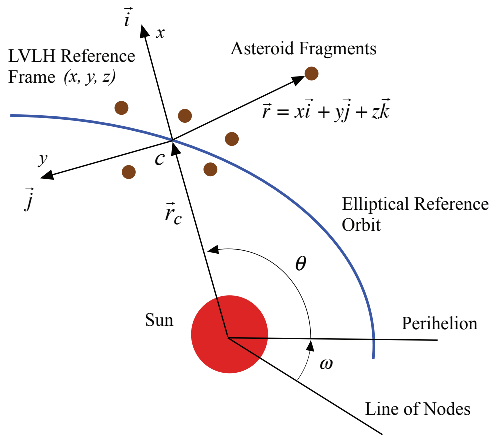

$\vec{i}$
x
LVLH Reference Frame (x, y, z)
Asteroid Fragments
$\vec{r} = x\vec{i} + y\vec{j} + z\vec{k}$
y
c
$\vec{j}$
$\vec{r}_c$
Elliptical Reference Orbit
θ
Sun
Perihelion
ω
Line of Nodes

Figure 6. Rotating Local Vertical Local Horizontal (LVLH) Frame.

$$\begin{aligned}
\ddot{x}_i &= 2\dot{\theta}\Big(\dot{y}_i - \frac{\dot{r}_c}{r_c}y_i\Big) + \dot{\theta}^2 x_i + \frac{\mu}{r_c^2} - \frac{\mu}{r_d^3}(r_c + x_i) + \frac{\mu_E(x_E - x_i)}{r_{Ei}^3} + \sum_j \frac{Gm_j(x_j - x_i)}{r_{ij}^3} \\
\ddot{y}_i &= -2\dot{\theta}\Big(\dot{x}_i + \frac{\dot{r}_c}{r_c}x_i\Big) + \dot{\theta}^2 y_i - \frac{\mu}{r_d^3}y_i + \frac{\mu_E(y_E - y_i)}{r_{Ei}^3} + \sum_j \frac{Gm_j(y_j - y_i)}{r_{ij}^3} \\
\ddot{z}_i &= -\frac{\mu}{r_d^3}z_i + \frac{\mu_E(z_E - z_i)}{r_{Ei}^3} + \sum_j \frac{Gm_j(z_j - z_i)}{r_{ij}^3}
\end{aligned} \tag{1}$$

where x_i, y_i, z_i, r_c, and θ are defined as shown in Figure 6; $r_d = |\vec{r}|$; G is the universal gravitational constant; and μ, μ_E, and μ_j are the solar gravitational parameter, Earth's gravitational parameter, and the gravitational parameter for each considered gravitating body. Finally, r_{Ei} is the relative distance between each fragment and the Earth, and r_{ij} is the relative distance between each fragment and the gravitating body being considered. The sum in each term contains the effects of all 3rd party gravitation besides that of Earth, and the positions of these bodies are computed at each time step as discussed in [6]. A fixed time step of 60 seconds is used in these computations to allow for all arrays to remain in GPU memory, rather than transferring the data to the host to determine an adaptive step size. The reason for this change will be discussed later in this paper.

Reentry Model

A density model was constructed based on a static Russian GOST atmosphere [15], with the coefficients listed in [6]. A static night-time atmosphere neglecting solar effects is assumed for altitudes above 120 km, using a solar flux value of $F_0 = 150$. This density then allows for a drag term to be added to the equation of motion, decelerating the fragment as it enters the atmosphere:

$$\dot{\mathbf{v}}_i = \dot{\mathbf{v}}_{ECI} - \frac{\rho(\mathbf{v}_i \cdot \mathbf{v}_i)SC_d}{2m_i}\hat{\mathbf{e}}_v \tag{2}$$

where $\dot{\mathbf{v}}_{ECI}$ is the acceleration of the fragment in the Earth Centered Inertial (ECI) frame, ρ is the density as a function of altitude, S is the exposed area, $\hat{\mathbf{e}}_v$ is the unit vector in the velocity direction, and $C_d = 1.7$ is the ballistic drag coefficient for a cylinder (the shape model assumed) [16]. Pressure stress and mass loss due to ablation are modeled using material parameters:

$$\dot{m}_i = -\frac{S}{Q} \min\left(\frac{1}{2} C_H \rho v_i^3, \sigma T^4\right) \tag{3}$$

where Q is the heat of ablation (assumed to be 1E7 J/m^3), C_H is the coefficient of heat transfer (assumed constant at 0.1), σ is the Stefan-Boltzmann constant, and T is the temperature of thermal ionization of the surrounding gas (25,000 K). This equation governs the ablative mass loss until the mean pressure in the cylinder $p = 0.25 C_d \rho v^2$ exceeds the yield strength of the material, at which point the energy deposition implies burnup of the fragment.

COMPUTATIONAL APPROACH

This section address the computational approach used to solved the problem. Each set of scaling and timing data is run separately from the others, allowing computation in parallel. The various sets of hardware used for computation and comparison are given. We present our model for host and GPU memory, and how we limited explicit communication along the hardware bus. Approached for limiting bandwidth use are discussed, followed by integrating multi-core CPU computation with the GPU executables.

Hardware and Implementation

A variety of hardware was available for this project, with a substantial difference in performance. This allowed us to get reasonable estimates on the computational cost of this simulation, in comparison to LINPACK performance numbers. Performance can vary based on the type of arrays used, and the number of threads dedicated to each GPU calculation. These factors are determined by the CUDA Compute Capability (CUDA CC), which is a property of the GPU [12]. These cost estimates are used to determine hardware performance on the various systems. A summary of the hardware used is shown in Table 2 (Note: all CPUs are Intel brand, and all GPUs are NVIDIA brand).

Table 2. Hardware for Benchmark Systems

System	Machine 1	Machine 2	Machine 3	Machine 4	Machine 5
CPU	1x Core2 Q6600	1x Core2 Q6600	1x Xeon X5550	2x Xeon E5520	2x Xeon X5650
CPU Cores	4	4	4	8	12
CPU TPEAK	9.6 GFLOPs	9.6 GFLOPs	12.8 GFLOPs	21.36 GFLOPs	32.04 GFLOPs
GPU	1x 8800GTS	1x GTX470	1x GTX480	4x Tesla c1060	4x Tesla c2050
GPU Cores	112	448	480	960	1792
GPU TPEAK	84 GFLOPs	324 GFLOPs	385 GFLOPs	336 GFLOPs	2060 GFLOPs
CUDA CC	CC 1.0	CC 2.0	CC 2.0	CC 1.3	CC 2.0

The implementation of the simulation is conducted in two ways. The first version uses CUDA extensions to the C language, and bindings for these kernels into existing Fortran 90 code. The second version uses CUDA Fortran, developed by the PGI group [17]. Since different sets of parameters are computationally independent of one another, one way to conduct parameter variation would be to have each computing thread handle a combined set of timing and scaling parameters, as shown in Figure 7. However, for memory management and to lower the amount of repeated calculations, we utilize the parallel nature of the fragments themselves as a basis for computation.

We fix a value for the timing parameters, allowing the nominal orbit to be calculated and shared among all versions of memory (discussed below). Then, looping through the velocity scaling parameter values, each thread on the GPU calculates the state variable change for one fragment, with the GPU kernel limited to one time step. This is necessary because the positions of the planets and other gravitating bodies must be calculated and transferred to the GPU at each time step. Reasons for this are discussed later in the paper. The final algorithm is shown in block diagram form in Figure 8.

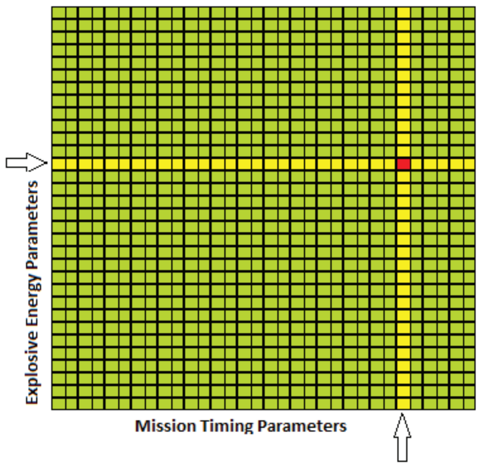

Figure 7. Visualization of Parameter Sweep Method.

Memory Model and Explicit Communication

Our memory model for this simulation includes a shared host memory, distributed device memory for each GPU, and data transfers between them handled through explicit array transfer. Each block of compute threads on the GPU takes the data it needs from the global device memory when the kernel reaches its block. This is an important factor, because hardware compute capabilities have different limitations on this block memory, changing the number of threads that may be used in the calculation. Constants are transferred to all GPU memories implicitly using a pointer to the host constant value. Figure 9 shows an overview of this computational memory model.

The explicit communication needed in the simulation for a single set of parameters is shown in the following psuedocode:

```
*Transfer state variable arrays Host to Device
Begin loop through time steps
    Calculate planetary positions at subintervals on host
    *Transfer planet position arrays Host to Device
    Launch GPU kernels to update state variables
    Calculate closest approach to Earth on GPU
    *Overwrite state arrays with Device to Device memory transfer
End time step loop
*Transfer final state back to Host, including close approach
Postprocessing on Host
```

Bandwidth Use and Serial Computation

One of the primary limitations of GPU acceleration is the PCI bus connecting the Host to the Device. Communication between these two sets of memory, or between individual GPUs, is therefore very expensive [12, 17]. Thus, the use of communication bandwidth should be minimized to achieve optimal performance. For example, an early implementation of a numerical integrator may be a subroutine that reads state variables from Host memory, computes the updated state on the GPU, and returns the next state to the Host. Unless the computation of the updated state is extremely intensive, this approach will not yield a high speedup over a CPU implementation. For smaller problems, the approach discussed above is preferred. Though the device code may be more complicated, this method was found to be an order of magnitude faster for an NEO

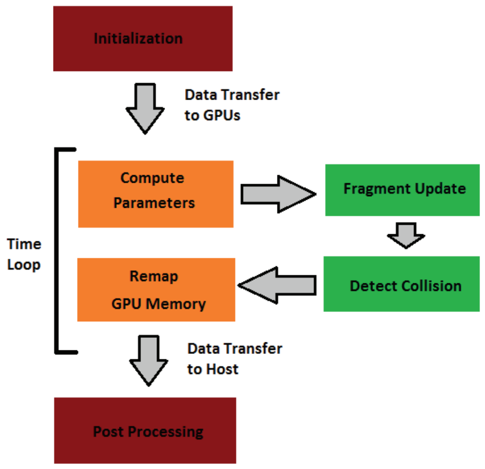

Figure 8. Block Diagram of Simulation Procedure.

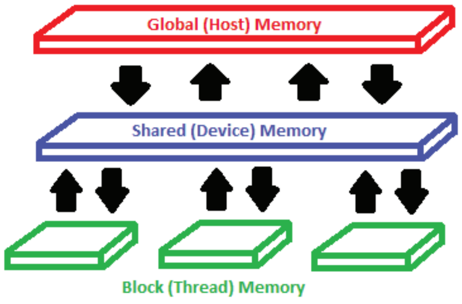

Figure 9. Visualization of Memory Model.

system with 18,220 fragments. With 511,744 fragments, the limitation from data transfer is less pronounced, though leaving arrays in device memory yielded a simulation that ran 5 times faster.

While modern dedicated compute GPUs have a high amount of onboard memory, it usually is far less than system memory. Though it may seem advantageous to calculate parameters for every time step before the start of the simulation, the resulting arrays can be quite large. Each model of GPU has a limited number of memory registers available to each computing block of threads [12]. Therefore, the use of several large arrays can actually slow down the simulation in some cases, by lowering the number of threads below the maximum allowed by the architecture. This trades off directly with the added expense of calculating parameters on the Host at each timestep. For the present work, calculating planetary positions at each step was found to be preferable to using a large pre-calculated array. For some hardware, sufficient GPU memory was not available.

Integration with SMP Computation

Some of the systems used to test this work had multiple GPUs. This was used to the advantage of the program by launching several Shared Memory Parallel (SMP) threads on the Host CPU. Each thread, or team of threads, was assigned a GPU on which to launch compute kernels. The calculations were conducted on portions of the state variable arrays. Since no interaction among fragments was assumed, the GPUs did not have to communicate the states of the fragments they were responsible for. This was found to be an extremely effective setup for large data sets, and scaled almost linearly to the number of GPUs used with some overhead for data transfer to partial arrays on the GPUs.

RESULTS

This section discusses the present results. Contours for sets of timing and scaling data are given, and we address the level of computation needed to obtain them. Computational speedup relative to CPU implementations are given for various codes used, and we briefly present our efforts at determining scalability of the present model. Finally, we address limitations unique to this type of architecture.

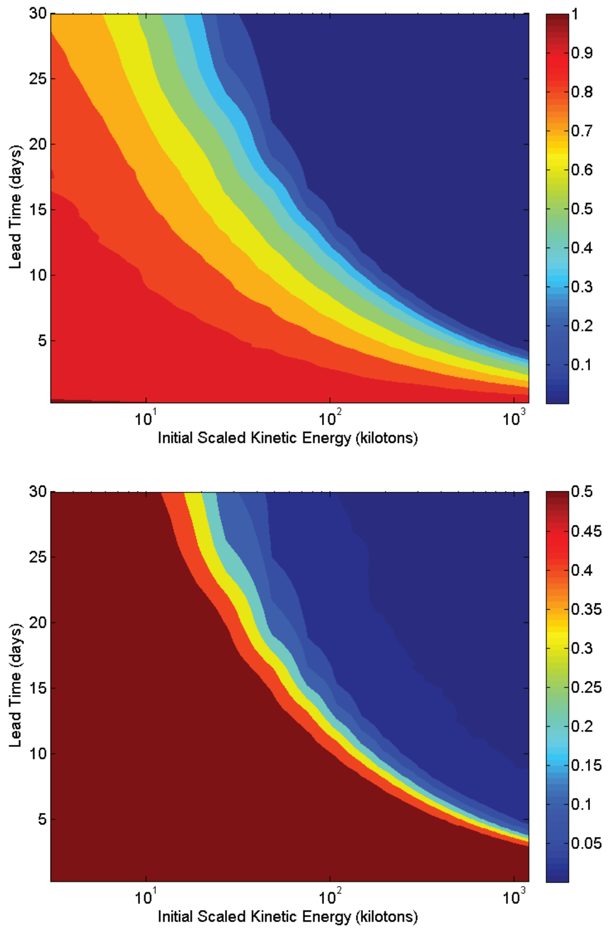

Figure 10. Impacting Mass Fraction Contours for Low Lead Time Cases.

Timing and Scaling Contours

A wide variety of timing and scaling parameters were investigated. Figure 10 shows the steep drop-off in impacting mass when both the available amount of time and the explosive power are increased for a range of up to 1.2 Mt and 30 days lead time. A different scale showing the contour for 0.5% of the initial mass is also given in Figure 10. The advantage to this approach over single parameter variation is that coupling between these two parameters can be observed. For example, If we take 1% of the initial impacting mass to be a measurement of success, then we can use the contour data to generate a relationship between lead time and the required explosive energy. A comparison of an analytical model and the data is shown in Figure 11. If L is the mission lead time and E is the required energy, this approximation is given by:

$$E = \exp\left(\text{-1.8401E-4}L^3 + \text{1.4826E-2}L^2 - \text{4.5491E-1}L + 9.9829\right) \tag{4}$$

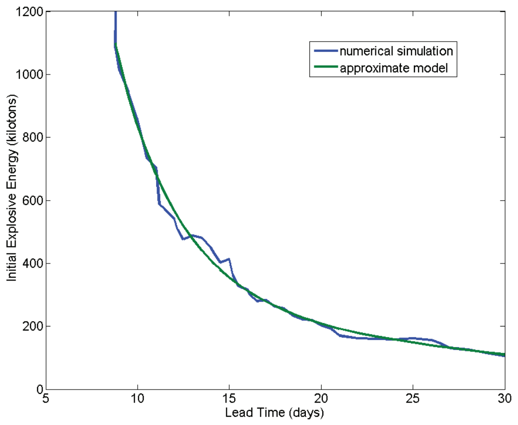

Figure 11. Analytical Approximation of Minimal Successful Mission Parameters.

The required explosive energy levels out below 200 kT as lead time increases. Therefore, even if a conventional explosive were to disrupt the target, it would not have enough initial kinetic energy to disperse the resulting fragments such that less than 1% of the initial mass remains on impacting trajectories.

Speedup and Scalability

Speedups of 20x to almost 80x were observed for an NEO disruption with 18,220 fragments. These are shown in Figure 12. The benefits of this approach for large data sets are also shown in Figure 12, in which an NEO system with over 500,000 fragments had computation speedups of up to 400x. This problem was found to be highly scalable, with multiple GPUs allowing large data sets to be broken up into manageable pieces. The speedup factors using Machine 5 on various data set sizes is shown in Figure 13.

Limitations and Future Work

One limitation of the present work is the need to compute system parameters at each time step. Surmounting this difficulty would yield large gains in performance by eliminating data transfers and serial computation at each step. The GPU computing model is not applicable to highly serial problems, and works best for distributed data sets like this fragmented NEO model. More applications of this technology continue to be discovered and applied.

The direct relationship between explosive yield and the initial velocities is unknown. Small yields may not be enough to entirely disrupt many NEOs, and further work in modeling subsurface explosions for these bodies must be done before a proof-of-concept mission with conventional explosives is feasible. Additionally, a better understanding of fragmentation under kinetic impact and various high-energy deflection methods is desired. Modeling and simulation with this understanding in mind is the subject of current work.

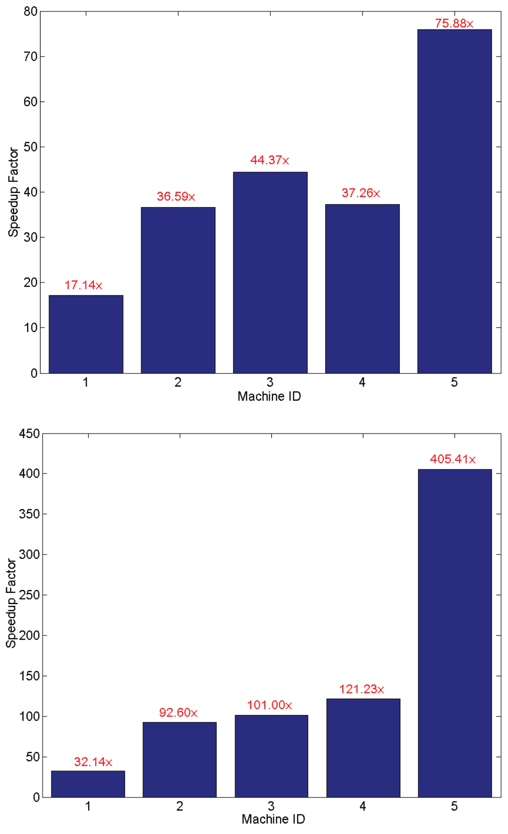

Figure 12. Computational Speedup Observed for Small and Large Data Sets.

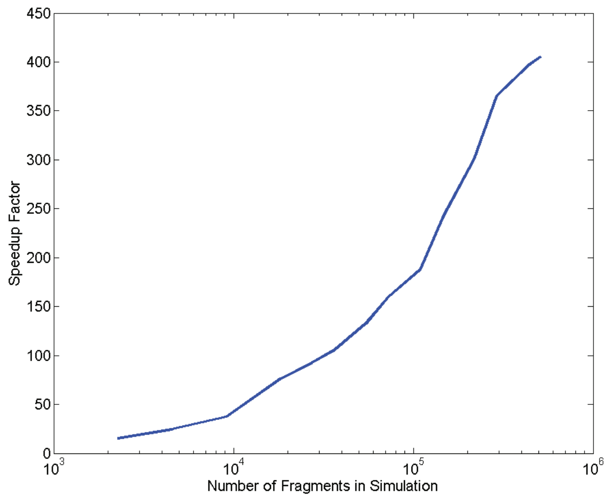

Figure 13. Computational Speedup for Varied Data Set Size (Machine 5).

CONCLUSION

Using the computational power of the GPU to accelerate NEO deflection simulation has resulted in an unprecedented capability for analysis of parameter variation. Reducing time to solution for problems with large data sets can allow millions of standard simulations to be compared. This will be essential for future optimization applied to mission design. A computational toolkit has been developed to allow coupling between mission design and mission effectiveness determination, through direct simulation using the design parameters.

Increased lead time was shown to be substantially effective in reducing needed explosive energy, but reduction below 200 kT resulted in very long lead times. These may not be feasible, even if the energy were sufficient to lead to fragmentation. Therefore, conventional disruption of a 270 m diameter target is not considered feasible at this time. Future work will analyze the fragmentation of smaller bodies to determine the possibility of a conventional proof-of-concept mission.

This technology has allowed larger data sets to be tested for NEO disruption simulation. A 511,744 fragment model of a 1 km body was test and shown to have a computational speedup of over 400x compared to serial implementation. The GPU accelerated simulation was shown to scale well to number of NEO fragments, achieving maximum speedup near the 511,744 fragment benchmark.

ACKNOWLEDGMENT

This research work was supported by a research grant from the Iowa Space Grant Consortium (ISGC) awarded to the Asteroid Deflection Research Center at Iowa State University. The authors would like to thank Dr. Ramanathan Sugumaran (Director, ISGC) for his support of this research work, and Professor Z.J. Wang for testing on his GPU server.

REFERENCES

[1] NASA Jet Propulsion Laboratory, Near Earth Object Program, http://neo.jpl.nasa.gov/neo/pha.html

[2] National Research Council, *Defending Planet Earth: Near-Earth Object Surveys and Hazard Mitigation Strategies*, Final Report, Committee to Review Near-Earth Object Surveys and Hazard Mitigation Strategies, The National Academies Press, January 2010.

[3] Kaplinger, B.D., and Wie, B., "A Study on Nuclear Standoff Explosions for Deflecting Near-Earth Objects," 1st IAA Planetary Defense Conference, April 2009.

[4] NASA/JPL Near-Earth Object Program Office, "Two Small Asteroids to Pass Close by Earth on September 8, 2010," http://neo.jpl.nasa.gov/news/news169.html, September 7, 2010.

[5] Wie, B., "Solar Sailing Kinetic Energy Impactor Mission Design for Impacting and Deflecting Near-Earth Asteroids" White Paper No. 009, presented at NASA Workshop on NEO Detection, Characterization, and Threat Mitigation, Vail, CO, June 26-29, 2006.

[6] Kaplinger, B.D., Wie, B., and Dearborn, D., "Preliminary Results for High-Fidelity Modeling and Simulation of Orbital Dispersion of Asteroids Disrupted by Nuclear Explosives," AIAA-2010-7982, AIAA/AAS Astrodynamics Specialists Conference, Toronto, Ontario, Canada, August 2-5, 2010.

[7] Dachwald, B., Kahle, R., and Wie, B., "Solar Sailing KEI Mission Design Tradeoffs for Impacting and Deflecting Asteroid 99942 Apophis," AIAA-2006-6178, AIAA/AAS Astrodynamics Specialist Conference, Keystone, CO, August 21-24, 2006.

[8] Wagner, S., and Wie, B., "Analysis and Design of Fictive Post-2029 Apophis Intercept Mission for Nuclear Disruption," AIAA-2010-8375, AIAA/AAS Astrodynamics Specialists Conference, Toronto, Ontario, Canada, August 2-5, 2010.

[9] Sanchez, J.P., Vasile, M., and Radice, G., "On the Consequences of a Fragmentation Due to a NEO Mitigation Strategy," IAC-08-C1.3.10, 59th International Astronautical Congress, Glasgow, UK., 29 Sept - 3 Oct., 2008.

[10] Kaplinger, B.D., Wie, B., and Dearborn, D., "Efficient Parallelization of Nonlinear Perturbation Algorithms for Orbit Prediction with Applications to Asteroid Deflection," AAS 10-225, 20th AAS/AIAA Space Flight Mechanics Meeting, San Diego, CA, February 15-17, 2010.

[11] Kirk, D.B., and W.W. Hwu, *Programming Massively Parallel Processors: A Hands-On Approach*, Morgan Kaufmann: Burlington, MA, 2010.

[12] NVIDIA Corporation, *NVIDIA CUDA C Programming Guide*, v3.1, May 28, 2010.

[13] NVIDIA Corporation, *OpenCL Programming Guide for the CUDA Architecture*, v3.1, May 26, 2010.

[14] Wie, B. and Dearborn, D., “Earth-Impact Modeling and Analysis of a Near-Earth Object Fragmented and Dispersed by Nuclear Subsurface Explosions,” AAS 10-137, 20th AAS/AIAA Space Flight Mechanics Meeting, San Diego, CA, February 15-17, 2010.

[15] Vallado, D.A., *Fundamentals of Astrodynamics and Applications*, Third Edition, Microcosm Press, Hawthorne, CA, 2007.

[16] Chyba, C.F., Thomas, P.J., and Zahnle, K.J., “The 1908 Tunguska Explosion: atmospheric disruption of a stony asteroid,” *Nature*, v361, p. 40-44, 1993.

[17] The Portland Group, *CUDA Fortran Programming Guide and Reference*, Release 2010.